NAUČNI ČLANCI
SCIENTIFIC PAPERS

COMPARISON OF DIFFERENT LATERAL ACCELERATION AUTOPILOTS FOR A SURFACE-TO-SURFACE MISSILE

Ćuk V. *Danilo*, University of Belgrade, Faculty of Mechanical Engineering, Department for Weapon Systems, Belgrade,
Mandić D. *Slobodan*, Ministry of Defence of the Republic of Serbia, Military Technical Institute, Division for Rocket Dynamics, Belgrade

UDC: 623.462.2 ; 629.7.051.5
FIELD: Mechanical engineering (Rocket technique)

Summary:

This paper presents a comparison of three lateral acceleration autopilots for a surface-to-surface missile: three-loop conventional acceleration autopilot, and gamma-dot and three-loop acceleration autopilot based upon the inverse-dynamic control. The surface-to-surface missile motion is described by nonlinear differential equations whose parameters change rapidly over a very wide range due to variable velocity and altitude. The requirement for the accurate controlling of the missile in such an environment represents a challenge for the autopilot designer. The brief review of the calculation of the autopilot gains is given using the concept of the "point" stability for the linear time-varying system with "frozen" dynamic coefficients. The method of the inverse-dynamic control is presented in the next section for two types of the autopilots: gamma-dot and acceleration autopilot. Both of them require the design of the estimators for the variables used as inputs to the control law. Finally, six-degree-of-freedom simulation results of the missile response to the demanded command on the typical ballistic trajectory are presented. The comparison of three autopilots considers the steady state errors and the sensitivity of the response to the highly variable environment. It was shown that the inverse-dynamic control can be very effective in the controlling of the surface-to-surface missile.

cukd@eunet.rs

Key words: *Autopilot, lateral Acceleration Autopilot, Gamma-dot Autopilot, Inverse-Dynamic Control, Guided Surface-to-Surface Missile, "Six-Degree-Of-Freedom" Model.*

Introduction

The aim of this paper is to present the main results of the comparison of different autopilot designs for a surface-to-surface missile (SSM). The free flight rocket designed to achieve the range about 50 km was modified to a guided weapon with reduced dispersion. The missile carries the flight computer, inertial measurement unit (IMU) with three rate gyros and three accelerometers, autopilot, and control section. The free flight rolling rocket was redesigned to canard a configuration whose control and guidance sections were stabilized against the rolling motion due to the application of the IMU and the strapdown navigation algorithm.

The purpose of the autopilot is to control the modified SSM during the whole flight, i.e., at low-, medium- and high altitude flight conditions. This is a difficult problem because the aerodynamic controls are very sensitive to the high variation of the air density, Mach number, angle of attack, and other missile dynamic properties needed for the autopilot design.

Typically, the design of the autopilot for the missile is based on the concept of the point stability technique. Most of the autopilots have a fixed structure whose gains are scheduled upon flight conditions such as dynamic pressure and the angle of attack. Therefore, tedious process of generating numerous aerodynamic transfer functions is required. After this step, the "frozen-point" stability is done to develop autopilot gains for the purpose of gain scheduling. This method of the autopilot design was described in many references such as Refs. [1], [2] and [3]. The authors of this paper have developed the computer codes for the complete numerical linearization of six-degree-of-freedom (6-DOF) model [4] and the autopilot design [5]. Different reference trajectories (ballistic, constant manoeuvre, straight line) were employed to generate aerodynamic transfer functions. One of the approaches in preparing the linear missile model based upon 6-DOF concept is shown in Ref. [6].

Many modern control methods with the application to the autopilot designs were published in papers, Refs. [7] – [10]. The method of the robust nonlinear inverse-dynamic control, or feedback linearization, [11] solves the problem of the synthesis of the autopilot for the missile having a highly varying nature. In addition to large variations in aerodynamics, mass, and inertia properties of a SSM, which occur during the boost phase, several constraints were faced by the autopilot designers. The problem of a small manoeuvre capability at high altitudes can be solved partially by allowance of small static instability (the centre of mass is behind

the centre of pressure). The Mach number is changed during the boost phase from the zero value to that greater than 3, when the static instability appears. The dynamic instability and dispersion for a free-flight rocket with extended range was analyzed in details in Ref. [12]. The robust control using the inverse-dynamic method can be applied to the SSM independently of the time instant on the trajectory even in the case of the dynamic instability [13].

In this paper, the results of different autopilot designs are discussed. The three-loop conventional acceleration autopilot is studied first. Using the concept of point stability, all necessary expressions for the autopilot's gains are rewritten from the published papers. The next section includes the method of the inverse-dynamic control and its application to two types of autopilots: gamma-dot and three-loop lateral acceleration autopilots. The numerical simulation results using a 6-DOF model will be presented to compare the SSM responses to the given commands on the trajectory for all three autopilot designs. Finally, some conclusions are given at the end of this paper.

The autopilot designs, presented in this paper, can be applied to both the missiles with Lambert guidance [14] and those without a thrust terminating mechanism [15].

Three-loop Conventional Acceleration Autopilot

Classical control techniques have dominated missile autopilot designs over the past several decades. Most missile autopilots employ acceleration and rate feedback with the proportional and integral control to stabilize the statically unstable missile and to track the guidance commands (Fig. 1).

The aerodynamic transfer functions of the pitch rate and normal acceleration to the controls deflections in Fig. 1 are, respectively

$$\frac{\Delta q}{\Delta \eta}(s) = \frac{K_q\left(T_q s + 1\right)}{T_n^2 s^2 + 2\varsigma_n T_n s + 1} \tag{1}$$

$$\frac{\Delta a_z}{\Delta q}(s) = -U_k \frac{T_\gamma^2 s^2 + 2\varsigma_\gamma T_\gamma s + 1}{T_q s + 1} \tag{2}$$

where

$$\begin{aligned} T_n^2 &= \frac{1}{\omega_n^2} = \frac{1}{-\left(m_w U_k - z_w m_q\right)} \\ 2\varsigma_n T_n &= \frac{m_q + z_w}{m_w U_k - z_w m_q} \end{aligned} \tag{3}$$

$$K_q = \frac{z_\eta m_w - z_w m_\eta}{m_q z_w - m_w U_k} \tag{4}$$

$$T_\gamma^2 = -\frac{z_\eta}{U_k\left(z_\eta m_w - z_w m_\eta\right)}$$
$$2\varsigma_\gamma T_\gamma = \frac{m_q z_\eta}{U_k\left(z_\eta m_w - z_w m_\eta\right)} \tag{5}$$

$U_k \approx V$ – missile velocity, z_w, – derivatives of linear acceleration with respect to the parameter in the subscript, m_w, m_q, m_η – derivatives of angular acceleration with respect to the parameter in the subscript, Ref. [16]. If the reference trajectory is ballistic, $\Delta q = q$, $\Delta a_z = a_z$, $\Delta\eta = \eta$.

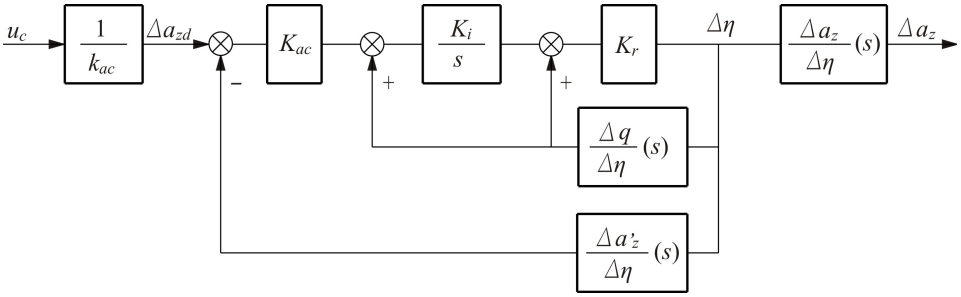

Figure 1 – Three-loop conventional acceleration autopilot

It is assumed that the acceleration is at the mass centre (CM), $\Delta a_z' = \Delta a_z$. If the accelerometer is away from the CM, the transfer function $\Delta a_z / \Delta q(s)$ has the same form, but the parameters T_γ^2 and $2\varsigma_\gamma T_\gamma$ should be modified as it was shown in [1] and [3]. From Fig. 1, the overall transfer function of the lateral acceleration to demanded acceleration can be developed as:

$$\frac{\Delta a_z}{\Delta a_{zd}}(s) = K\frac{T_\gamma^2 s^2 + 2\varsigma_\gamma T_\gamma s + 1}{\frac{T_n^2}{K_0}s^3 + \left(\frac{2\varsigma_n T_n}{K_0} + T_0^2\right)s^2 + \left(\frac{1}{K_0} + 2\varsigma_0 T_0\right)s + 1} \tag{7}$$

where

$$K_0 = -K_r K_i K_q\left(1 + K_{ac} U_k\right) \tag{8}$$

$$T_0^2 = \frac{T_\gamma^2 + \dfrac{T_q}{K_{ac}U_k K_i}}{1 + \dfrac{1}{K_{ac}U_k}} \tag{9}$$

$$2\varsigma_0 T_0 = \frac{2T_\gamma\varsigma_\gamma + \dfrac{T_q + \dfrac{1}{K_i}}{K_{ac}U_k}}{1 + \dfrac{1}{K_{ac}U_k}} \tag{10}$$

$$K = \frac{1}{1 + \dfrac{1}{K_{ac}U_k}} \tag{11}$$

The gains of the autopilot K_{ac}, K_r, K_i, should be chosen in such a way to provide the desired parameters of the closed loop τ_e, ω_e, ς_e:

$$\frac{\Delta a_z}{\Delta a_{z_d}}(s) = K\frac{T_\gamma^2 s^2 + 2\varsigma_\gamma T_\gamma s + 1}{(\tau_e s + 1)\left(\dfrac{s^2}{\omega_e^2} + \dfrac{2\varsigma_e}{\omega_e}s + 1\right)} \tag{12}$$

Instead of the required value for ω_e, we usually define the open-loop cross-over frequency $\omega_c \approx (2-3)\omega_n$ where $\omega_n = 1/T_n$ is the missile natural frequency.

Equating the corresponding coefficients in the denumerators of Eqs. (12) and (7) gives the following expressions for the autopilot gains:

$$K_i = \frac{T_0^2 - T_\gamma^2 - T_q\left(2\varsigma_0 T_0 - 2T_\gamma\varsigma_\gamma\right)}{\left(2\varsigma_0 T_0 - T_q\right)\left(T_0^2 - T_\gamma^2\right) - T_0^2\left(2\varsigma_0 T_0 - 2T_\gamma\varsigma_\gamma\right)} \tag{13}$$

$$K_{ac} = \frac{1}{U_k}\frac{T_0^2 - \dfrac{T_q}{K_i}}{T_\gamma^2 - T_0^2} \tag{14}$$

$$K_r = \frac{K_0}{-K_q K_i\left(1 + K_{ac}U_k\right)} \tag{15}$$

In a general case, the steady state gain $\neq 1$. Therefore, the pre-gain $k_{ac} = K$ may be required to achieve the demanded acceleration.

Autopilot Design Using Inverse-Dynamic Control

Theoretical Background

This section follows the description of the inverse-dynamic control given in Ref. [13]. The missile's nonlinear equations of motion can be separated into a nonlinear homogeneous term plus the term which is the linear function of the control vector

$$\dot{\mathbf{x}} = \mathbf{f}(\mathbf{x}) + \mathbf{G}(\mathbf{x})\mathbf{u} \tag{16}$$

where $\mathbf{x}$ is a $n \times 1$ state vector and $\mathbf{u}$ is the control vector of the dimension $m \times 1$; $\mathbf{G}(\mathbf{x})$ is $n \times m$ matrix of control sensitivity. We assume that the $m \times 1$ output vector $\mathbf{y}$ is a linear function of the state vector

$$\mathbf{y} = \mathbf{H}\mathbf{x} \tag{17}$$

The matrix $\mathbf{H}$ is selected by the designer. The derivative of the chosen output vector is:

$$\dot{\mathbf{y}} = \mathbf{H}\dot{\mathbf{x}} = \mathbf{H}[\mathbf{f}(\mathbf{x}) + \mathbf{G}(\mathbf{x})\mathbf{u}] \cong \mathbf{f}^*(\mathbf{x}) + \mathbf{G}^*(\mathbf{x})\mathbf{u} \tag{18}$$

where $\mathbf{f}^*(\mathbf{x})$ and $\mathbf{G}^*(\mathbf{x})$ have dimensions $m \times 1$ and $m \times m$, respectively. Denoting the derivative of $\mathbf{y}$ as $\mathbf{v}$

$$\dot{\mathbf{y}} = \mathbf{v} \tag{19}$$

the inverting control law is obtained

$$\mathbf{u} = \mathbf{G}^{*-1}(\mathbf{x})[\mathbf{v} - \mathbf{f}^*(\mathbf{x})] \tag{20}$$

The control law includes a model of missile's homogeneous dynamics in the feedback loop and the inverse of its control effects in the forward loop (Fig. 2). The final step is to design a controller for the system described by Eq. (19).

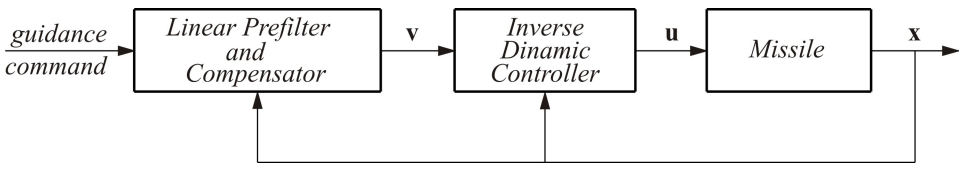

Figure 2 – Inverse dynamic control

The matrix $\mathbf{G}^*(\mathbf{x}) = \mathbf{HG}(\mathbf{x})$ is often not invertible because some elements of $\mathbf{y}$ are not linear functions of $\mathbf{u}$. The repeated differentiation eventually reveals a linear relationship. Suppose that this can be applied to the first element of $\mathbf{y}$, i.e., y_1

$$\dot{y}_1 = \mathbf{h}_1\mathbf{f}(\mathbf{x}) \tag{21}$$

where $\mathbf{h}_1$ is the first row of $\mathbf{H}$. The second derivative of y_1 is

$$\ddot{y}_1 = \mathbf{h}_1\dot{\mathbf{f}}(\mathbf{x}) = \mathbf{h}_1\frac{\partial\mathbf{f}(\mathbf{x})}{\partial\mathbf{x}}[\mathbf{f}(\mathbf{x}) + \mathbf{G}(\mathbf{x})\mathbf{u}] \tag{22}$$

If the necessary linear relationship between $\mathbf{u}$ and $\ddot{y}_1$ is established, the first rows of $\mathbf{f}^*(\mathbf{x})$ and $\mathbf{G}^*(\mathbf{x})$ are redefined as $\mathbf{h}_1\frac{\partial\mathbf{f}(\mathbf{x})}{\partial\mathbf{x}}\mathbf{f}(\mathbf{x})$ and $\mathbf{h}_1\frac{\partial\mathbf{f}(\mathbf{x})}{\partial\mathbf{x}}\mathbf{G}(\mathbf{x})$, respectively.

The second element of $\mathbf{y}$ is checked then. If Eq. (22) does not produce a linear relationship, the next derivative of y_1 is generated. We denote the vector of suitable derivatives of $\mathbf{y}$ by $\mathbf{y}^{(d)}$, and $\mathbf{f}^*(\mathbf{x})$ and $\mathbf{G}^*(\mathbf{x})$ are defined row by row. Hence,

$$\mathbf{y}^{(d)} = \mathbf{f}^*(\mathbf{x}) + \mathbf{G}^*(\mathbf{x})\mathbf{u} \tag{23}$$

where $\mathbf{G}^*(\mathbf{x})$ is invertible for linearly independent controls. If $\mathbf{v}$ represents the desired values of $\mathbf{y}^{(d)}$, the inverting control is described by Eq. (20). The application of the inverse control can be complex because the evaluation of $\mathbf{f}^*(\mathbf{x})$ and $\mathbf{G}^*(\mathbf{x})$ requires that a full, $d-$differentiable model of the missile be included in the control system. It is worth to say that the inverse-dynamic control can be applied to both nonlinear and linear time-varying systems.

Gamma – Dot Autopilot

The gamma-dot autopilot is used to control the velocity vector turn rate, $\dot{\gamma}$. It is useful in the case of SSM with proportional navigation because it provides explicit control of the missile velocity vector turn rate required by the guidance law. If the missile has the pitch and yaw rate gyros for measuring body rates, an estimator is implemented to reconstruct the missile gamma-dots. The error in estimating the gamma-dots depends on the errors in estimating missile's aerodynamic characteristics. In the ca-

se of full strapdown navigation systems, the gamma-dots and all the other parameters required by the autopilot are generated using a navigation algorithm. Since the pitch and yaw channels are identical, only the former will be described.

Using notations in Fig. 3, we can develop a simplified model for missile's motion. The velocity vector turn rate is given by

$$\dot{\gamma} = -\frac{(Z + Z_c)\cos\alpha}{mV} + \frac{F_x - X}{mV}\sin\alpha \tag{24}$$

where Z, Z_c F_x, X, m are normal force due to angle-of-attack and controls deflection, thrust, aerodynamic axial force, and missile mass, respectively.

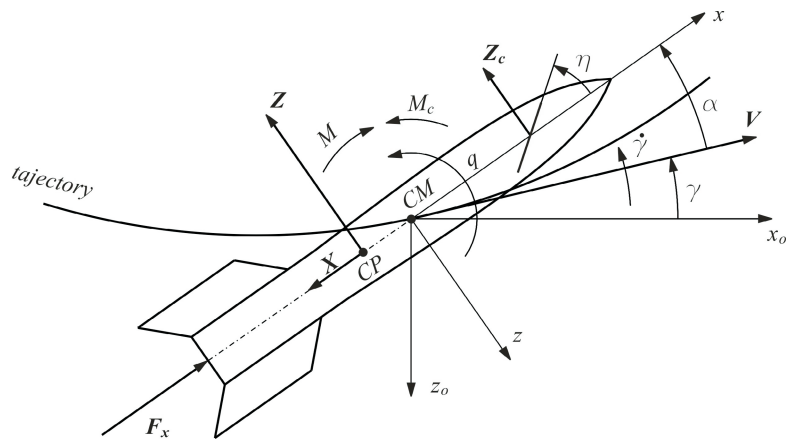

Figure 3 – Forces and moments acting on the missile

Substituting the following approximations

$$\begin{aligned} &Z = Z_\alpha \alpha,\ Z_c = Z_\eta \eta,\ M = M_\alpha \alpha, M_c = M_\eta \eta, \\ &a_x = \frac{F_x - X}{m},\ \sin\alpha \approx \alpha,\ \ \cos\alpha \approx 1,\ \ \eta = -\frac{m_\alpha}{m_\eta}\alpha \end{aligned} \tag{25}$$

into Eq. (24), we get

$$\dot{\gamma} = f_\alpha \alpha \tag{26}$$

where

$$f_\alpha = \frac{\partial \dot{\gamma}}{\partial \alpha} = -\frac{1}{V}(z_\alpha - z_\eta \frac{m_\alpha}{m_\eta}) + \frac{a_x}{V} \tag{27}$$

$$z_\alpha = \frac{Z_\alpha}{m} = Vz_w,\ z_\eta = \frac{Z_\eta}{m},\ m_\alpha = \frac{M_\alpha}{I_y} = Vm_w,\ m_\eta = \frac{M_\eta}{I_y}, \tag{28}$$

We select the following state variables:

$$x_1 = \dot{\gamma} \tag{29}$$

$$x_2 = q \tag{30}$$

Using the kinematical relationship

$$\dot{\alpha} = q - \dot{\gamma} \tag{31}$$

after differentiating Eqs. (29) and (30), we get

$$\dot{x}_1 = f_\alpha \left(q - f_\alpha \alpha\right) + \dot{f}_\alpha \alpha \tag{32}$$

$$\dot{x}_2 = m_\alpha \alpha + m_\eta \eta \tag{33}$$

Now, we can implement the method of the inverse-dynamic control. The estimated quantity $\dot{\gamma}$ will be a controlled variable. After an additional differentiating step in Eq. (32) and introducing the new state variables

$$y_1 = x_1 = \dot{\gamma} \tag{34}$$

$$y_2 = \dot{x}_1 \tag{35}$$

we get the transformed system of differential equations

$$\dot{y}_1 = y_2 \tag{36}$$

$$\dot{y}_2 = v \tag{37}$$

where

$$v = f_\alpha \left[m_\alpha \alpha + m_\eta \eta - f_\alpha (q - f_\alpha \alpha) - \dot{f}_\alpha \alpha \right] + 2\dot{f}_\alpha (q - f_\alpha \alpha) + \ddot{f}_\alpha \alpha \tag{38}$$

The new system described by Eqs. (36) and (37) is a linear, time-invariant system with a new control input v. The deflection of control surfaces may be easily determined from Eq. (38) in terms of the new control input v and the parameters of missile motion.

The control law for the new time-invariant system can be defined to satisfy some design requirements

$$v = C_0 \left[\tau(\dot{\gamma}_c - y_1) + \int (\dot{\gamma}_c - y_1) dt \right] - C_2 y_2 - C_1 y_1 \tag{39}$$

where $\dot{\gamma}_c$ is the demanded value of the velocity vector turn rate and $y_1 = \dot{\gamma}$. The coefficients C_0, C_1, C_2 and the time constant τ may be

defined through the synthesis of the autopilot. The application of Laplace transformation in Eqs. (36), (37) and (39) and solving for $y_1 = \dot{\gamma}$ in terms of demanded input $\dot{\gamma}_c$ gives the transfer function of the overall time-invariant system

$$\frac{\dot{\gamma}}{\dot{\gamma}_c}(s) = \frac{C_0(\tau s + 1)}{s^3 + C_2 s^2 + (C_1 + \tau C_0)s + C_0} = \frac{C_0(\tau s + 1)}{s^3 + C_2 s^2 + C_1' s + C_0} \tag{40}$$

Equation (38) can be solved for the deflection of controls as

$$\eta = K_\gamma[\tau(\dot{\gamma}_c - \dot{\gamma}) + \int(\dot{\gamma}_c - \dot{\gamma})dt - K_r q - K_\alpha \alpha + \eta_{cor}(t) \tag{41}$$

where

$$K_\gamma = \frac{C_0}{f_\alpha m_\eta} \tag{42}$$

$$K_r = \frac{C_2 - f_\alpha}{m_\eta} \tag{43}$$

$$K_\alpha = \frac{1}{m_\eta}\left(C_1' + m_\alpha - K_r f_\alpha m_\eta - K_\gamma \tau f_\alpha m_\eta\right) \tag{44}$$

$$\eta_{cor}(t) = -\frac{1}{f_\alpha m_\eta}\left[\ddot{f}_\alpha - \dot{f}_\alpha(-C_2 + 3f_\alpha)\right]\alpha - \frac{2\dot{f}_\alpha}{f_\alpha m_\eta} q \tag{45}$$

The block-diagram of the gamma-dot autopilot is shown in Fig. 4. The deflection of controls depends on the measured value of the pitch rate q, estimated values of $\hat{\dot{\gamma}}, \hat{\alpha}$, and the additional correction $\eta_{cor}(t)$ which is the consequence of the variable velocity vector turn rate derivative $f_\alpha(t)$. If $\dot{f}_\alpha = \ddot{f}_\alpha = 0$, the correction to the deflection of controls is equal to zero.

The coefficients C_0, C_1', C_2 are defined by the placement of the closed-loop poles, while the time constant τ is selected to compensate for the aperiodic time lag in the autopilot loop.

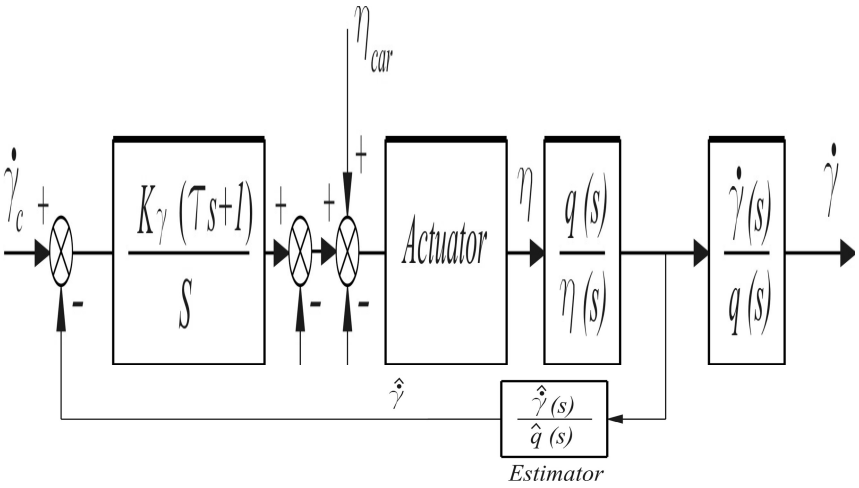

Figure 4 – Gamma-dot autopilot

Three-Loop Acceleration Autopilot

The inverse-dynamic control will be applied to the three-loop acceleration autopilot as well. Instead of using the velocity turn rate $\dot{\gamma}$ as a state variable, the normal acceleration is introduced

$$a_n = -V\dot{\gamma} = -Vf_\alpha\alpha = g_\alpha\alpha \cong x_1 \tag{46}$$

Since the second state variable remains the pitch rate ($x_2 = q$), the simplified state space model takes the following form:

$$\dot{x}_1 = \dot{g}_\alpha\alpha + g_\alpha\dot{\alpha} \tag{47}$$

$$\dot{x}_2 = m_\alpha\alpha + m_\eta\eta \tag{48}$$

$$\dot{\alpha} = q - \dot{\gamma} = q + \frac{a_n}{V} \tag{49}$$

The controlled variable is normal acceleration, $y_1 = a_n$. Taking two differentiations on the normal acceleration and defining new variables in the transformed system, $y_1 = a_n, y_2 = \dot{a}_n$, we get again:

$$\dot{y}_1 = y_2 \tag{50}$$

$$\dot{y}_2 = v \tag{51}$$

where

$$v = 2\dot{g}_\alpha \left(q + \frac{a_n}{V} \right) + \ddot{g}_\alpha \alpha + g_\alpha \left[m_\alpha \alpha + m_\eta \eta - g_\alpha \left(q + \frac{a_n}{V} \right) - g_\alpha \alpha \right] \quad (52)$$

Hence, we get the time-invariant system and the design of the optimal autopilot can be done easily. Again, after two differentiations the linear function with respect to the deflection of controls in the expression for a new control input v, Eq. (52), is obtained.

The integral control law was applied

$$v = C_0 \int (a_{nc} - y_1) dt - C_2 y_2 - C_1 y_1 \quad (53)$$

The transfer function of the normal acceleration $y_1 = a_n$ to the demanded value of the normal acceleration a_{nc} follows from Eqs. (50), (51) and (53):

$$\frac{a_n}{a_{nc}}(s) = \frac{C_0}{s^3 + C_2 s^2 + C_1 s + C_0} \quad (54)$$

The D.C. gain is equal to unity, and the zero steady-state error occurs. From Eqs. (50) and (51), with the new controlled variable given by Eq. (53), the solution of Eq. (52) for the controls deflection η gives:

$$\eta = K_{ac} \int (a_{nc} - a_n) dt - K_r q - K_\alpha \alpha + \eta_{cor}(t) \quad (55)$$

where

$$K_{ac} = \frac{C_0}{V f_\alpha m_\eta} \quad (56)$$

$$K_r = \frac{1}{m_\eta}(C_2 - f_\alpha) \quad (57)$$

$$K_\alpha = \frac{1}{m_\eta}(C_1 + m_\alpha - K_r f_\alpha m_\eta) \quad (58)$$

$$\eta_{cor}(t) = -\frac{1}{g_\alpha m_\eta}\left[\ddot{g}_\alpha + \dot{g}_\alpha (K_r m_\eta - f_\alpha) - g_\alpha \dot{f}_\alpha \right] \alpha - \frac{2\dot{g}_\alpha}{g_\alpha m_\eta} q \quad (59)$$

The control law of the three-loop acceleration autopilot generated by the inverse-dynamic control is similar to that of the gamma-dot autopilot. In order to obtain a linear time-invariant system, instead of the pitch angle feedback as in the case of the conventional acceleration autopilot, we need the angle-of-attack feedback [see Eq. (55)]. The autopilot is desig-

ned by using the estimator for the angle-of-attack. The compensation of the rapid changes in g_α is introduced via the corrected value of the control deflection $\eta_{cor}(t)$, Eq. (59).

Numerical Examples and Simulation

To determine the response of the missile having different autopilot designs, the six-degree-of-freedom model and numerical simulation were applied. The missile configuration used in the simulation study is an artillery rocket of the range about 50 km. The aspect ratio of the body is $l/d = 17{,}8$. The canard section is built into the nose section inside the diameter of the cylindrical body at the distance of $l/d = 1{,}55$ from the missile tip. The fin-stabilized configuration has four pop-out fins without cant for generating the rolling motion. The roll autopilot is used to stabilize the canard section with the IMU against the rolling motion. The rocket motor having the total impulse of 33500 dNs imparts the velocity over Mach 3 to the missile to achieve the range over 50 km. The motor has two levels of the thrust 27800/8000 dN with burn times of 0.17/3.80 sec. The missile weight, the mass centre location from the missile tip, the roll and the transverse inertia radius before and after burn is 390/225 kg, 2.65/2.47 m, 0.094/0.098 and 1.2/1.4 m, respectively. The elevation angle of 54.19 deg was chosen to achieve the range of 50 km. The apogee of the trajectory is 19600 m. The aerodynamic data for the 6-DOF model were generated by numerical simulation and wind tunnel tests.

The missile configuration is statically unstable in the time interval $t \in (3{,}9;5{,}1)$ s when a high value of the Mach number is achieved. Two control points were selected for the autopilot design: $t = 10$ s (after the burn out time when the missile becomes statically stable again), and $t = 60$ s (near to the apogee of the trajectory).

Using the "frozen'' aerodynamic transfer functions parameters for $t = 10$ s and the desired autopilot's dynamics given by

$$\omega_c = 3\omega_n = 3 \times 5{,}35 \approx 15 \text{ rad/s},\ \varsigma_e = 0{,}6,\ \tau_e = 0{,}1 \text{ s} \tag{60}$$

the gains of the three-loop conventional autopilot were calculated by Eqs. (11) - (15):

$$K_{ac} = 0{,}012 \text{ s/m},\ K_i = 3{,}58 \text{ 1/s},\ K_r = 0{,}647 \text{ s},\ k_{ac} = 0{,}91 \tag{61}$$

The responses of the autopilot to the demanded unit step input for $t = 3, 5, 10, \text{ and } 15$ s are shown in Fig. 5. The time varying transfer functions parameters have important effects on the autopilot's responses

which are characterized by an increased dynamic errors if the time is different from the point selected for the design.

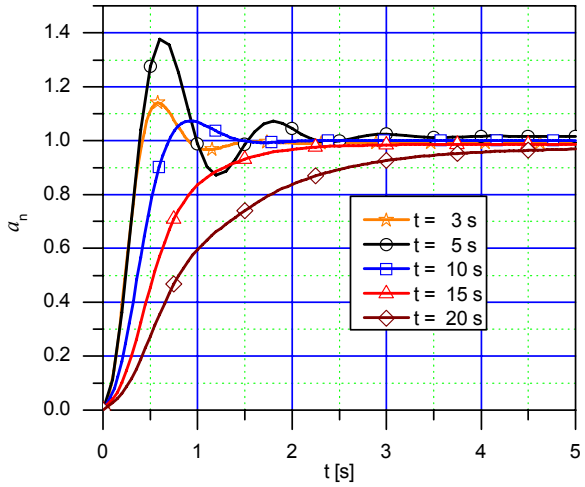

Figure 5 – Responses of a conventional autopilot designed for t=10 s

The response of the missile to the given command of $\pm 1\ \mathrm{g}$ by using the 6-DOF model for the gains in Eq. (61) is shown in Figs. 6 and 7 for the normal acceleration and the deflection of controls and angle-of-attack, respectively. A more realistic numerical simulation by the 6-DOF model shows that the satisfactory autopilot response was not obtain even in the vicinity of the chosen control point, $t = 10\ \mathrm{s}$. The additional adjustment of the autopilot is required. The change of the gain K_{ac} to the value of $K_{ac} = 0.02$ gives the response with the reduced steady state error, but with the increased overshoot, as shown in Fig. 8. The concept of the „frozen“ point stability in the design of the three-loop conventional acceleration autopilot cannot give good results for the wide interval of the missile flight.

The identical procedure was repeated for the control point near to the apogee of the trajectory, $t = 60\ \mathrm{s}$. Since the natural frequency of the missile is reduced to $\omega_n = 2\ \mathrm{rad/s}$, the desired values of the autopilot dynamics were chosen to be $\omega_c = 6\ \mathrm{rad/s}$, $\tau_e = 0{,}5\ \mathrm{s}$, $\varsigma_e = 0{,}6$. The new values of the autopilot gains were obtained as $K_{ac} = 0{,}057\ \mathrm{s/m}$, $K_i = 2{,}49\ 1/\mathrm{s}$, $K_r = 2{,}93\ \mathrm{s}$, $k_{ac} = 0{,}96$. The results of the numerical – simulation by the 6-DOF model in Fig. 9 show again that the additional

adjustments of the gains are useful. Since the manoeuvre capability of the SSM is highly reduced at the apogee, the demanded acceleration was ± 0.1 g.

The gamma-dot autopilot was designed using the inverse dynamic control for the same desired dynamic characteristics as those for a conventional autopilot at t=10 s, Eq. (60). Based on these values, the coefficients in the transfer function Eq. (40) were calculated as $\tau = \tau_e = 0.1$ s, $C_0 = 260$, $C_1' = 87$, $C_2 = 16$. Eqs. (42) – (45) were used for the calculation of the autopilot gains and the correction of the controls deflection due to time varying dynamics needed for the control law, defined by Eq. (41). Fig. 10 illustrates the autopilot response to a step command ± 1 deg/s.

In comparison to the conventional autopilot, the gamma-dot autopilot shows better performances because the desired dynamics was achieved without steady state errors. For the same desired dynamics as in the case of the conventional autopilot at t=60 s, the response to the demanded value of the velocity vector turn rate of $\pm 0{,}1$ deg/s is shown in Fig. 11. The comparison of the diagrams in Figs. 9 and 11 proves some advantages of the gamma-dot over the conventional autopilot: faster response and lower values of dynamic errors in tracking the demanded velocity vector turn rate.

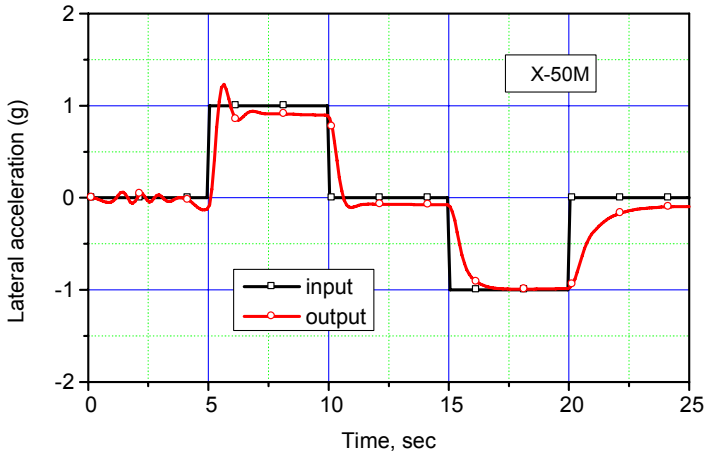

Figure 6 – Three-loop conventional acceleration autopilot ($t = 10$ s, $K_{ac} = 0.012$)

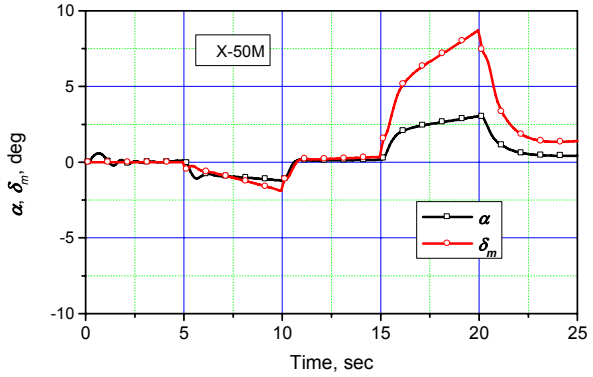

Figure 7 – Three-loop conventional acceleration autopilot
($t = 10$ s, $K_{ac} = 0.012$ s/m, $\delta_m \cong \eta$)

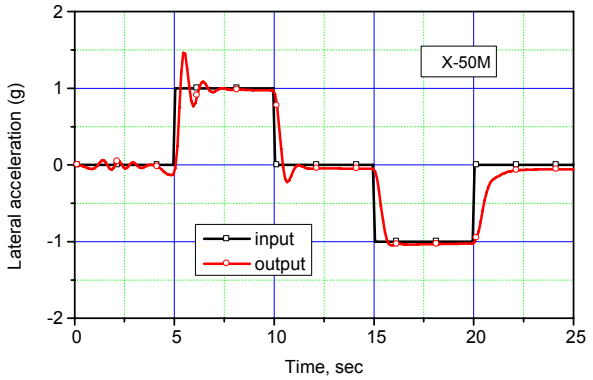

Figure 8 – Three-loop conventional acceleration autopilot
($t = 10$ s, $K_{ac} = 0.02$ s/m)

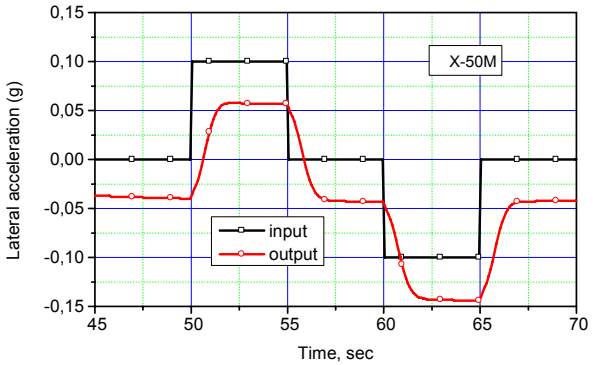

Figure 9 – Three-loop conventional acceleration autopilot
($t = 60$ s, $K_{ac} = 0.057$ s/m)

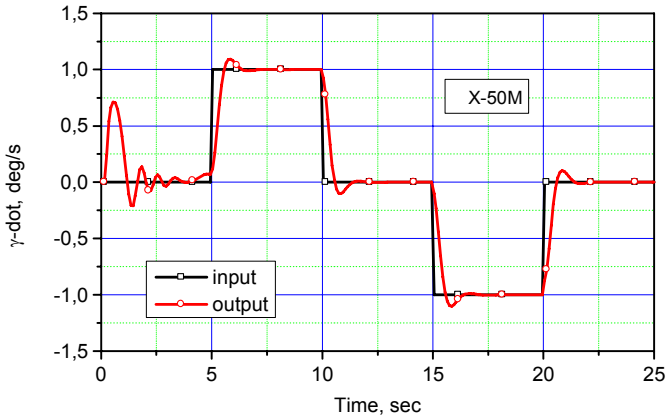

Figure 10 – Gamma-dot autopilot (design point $t = 10$ s)

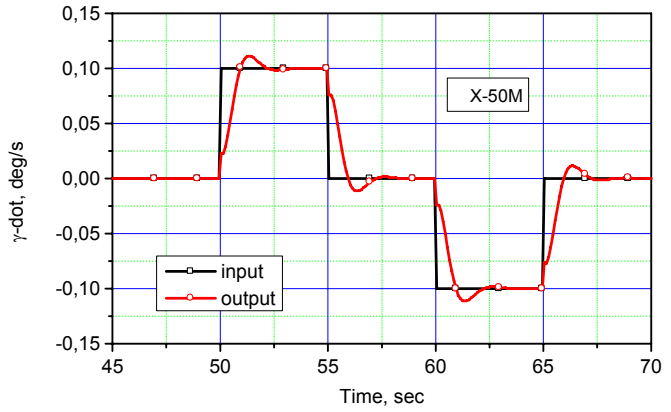

Figure 11 – Gamma-dot autopilot (design point $t = 60$ s)

The design of the three-loop acceleration autopilot was done using the inverse-dynamic control and having the identical requirements at the control points $t = 10$ s and $t = 60$ s as in the examples of the conventional and gamma-dot autopilot. The corresponding responses in Figs. 12 and 13 show that good performances can be achieved with this autopilot. The slower responses were obtained in the comparison with the gamma-dot autopilot because the control law Eq. (55) has only integral of the difference between the demanded signal and the output signal. In spite of time varying missile dynamics, the quality of the transient response does not change with the flight time.

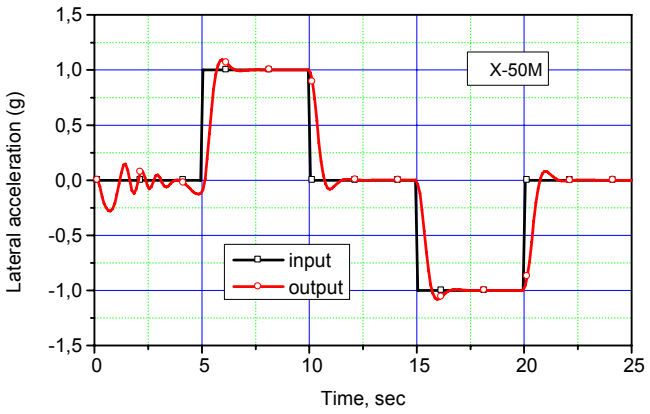

Figure 12 – Three-loop acceleration autopilot designed by the inverse-dynamic control ($t = 10$ s)

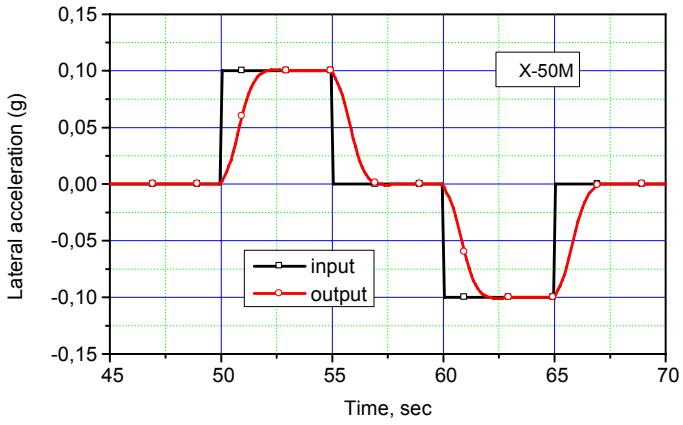

Figure 13 – Three-loop acceleration autopilot designed by the inverse-dynamic control ($t = 60$ s)

Conclusion

Three types of lateral acceleration autopilots for a surface-to-surface missile were analyzed: three-loop conventional acceleration autopilot, and gamma-dot and three-loop acceleration autopilot based upon the application of the inverse-dynamic control. The design of the first one employs the concept of the point stability for the system with "frozen" aerodynamic transfer functions. After the calculation of the autopilot gains for the full envelope of the missile flight, the additional adjustment of the gains should be done to compensate for the time varying dynamics of

the SSM. Contrary to this method, the inverse-dynamic control is well suited for the controlling of a missile with the rapidly time-varying dynamics as in the case of a surface-to-surface missile. However, its application requires the design of the estimators for the velocity vector turn rate and the angle-of-attack. The synthesis of such an autopilot begins with the choice of the pre-filter and the compensator for the linear time-invariant system. After this step, the calculation of the controls deflection in terms of the defined new control input and the missile measured or estimated parameters of motion should be done. The gamma-dot and three-loop acceleration autopilot, designed by the inverse-dynamic control, demonstrate excellent performances – fast response and zero steady state errors in a rapidly time varying environment of the SSM. This was proved by the numerical simulation results using a 6-DOF model for the missile flight to the range of 50 km.

There are still some questions to be investigated and solved. It is recommended that research be continued by the design of the required estimators, including the study of the influence of the missile dynamics uncertainties on the autopilot response.

References

[1] Nesline, F.W., Nesline, M.L., *How Autopilot Requirements Constrain the Aerodynamic Design of Homing Missiles*, AIAA Guidance and Control Conference, TA7, 1983, pp. 716-730.

[2] Gazzina, A., *How to Control Missile Airframes: Methodology and Limitation,* AGARD-CP-451, Stability and Control of Tactical Missile Systems, 1989, pp. 13.1–13.8.

[3] Ćuk, D., Mandić, S., *Pitch Autopilot Design for a Missile with Highly Non-Stationary Dynamical Parameters*, Scientific Technical Review, Military Technical Institute, Belgrade, 3/2000.

[4] Ćuk, D., Ćurčin, M., Mandić, S., *GMTC_3D: Guided Missile Trajectory Calculation – Three Degree of Freedom Motion Model, Theoretical Manual,* Military Technical Institute, Belgrade, 2002.

[5] Ćuk, D., Ćurčin, M., Mandić, S., *Autopilot Design, Theoretical Manual,* Military Technical Institute, Belgrade, 2004.

[6] Bar-on, J. R., Adams, R. J., *Linearization of a Six-Degree-of-Freedom Missile for Autopilot Analysis,* J. Guidance, 1/1998, pp. 184–187.

[7] Arrow, A., Williams, D. E., *Comparison of Classical and Modern Autopilot Design and Analysis Techniques,* J. Guidance, 2/1989, pp. 220–227.

[8] Puri, N. N., *Design of an Optimal-Adaptive Digital Autopilot,* J. Spacecraft, 7/1970, pp. 1172–1176.

[9] Buschek, H., *Full Envelope Missile Autopilot Design Using Gain Scheduled Robust Control,* Journal of Guidance, Control, and Dynamics, 1/1999, pp. 115–128.

[10] Zhu, J. J., Mickle, M. C., *Missile Autopilot Design using a New Linear Time-Varying Control Technique,* Journal of Guidance, Control, and Dynamics, 1/1997, pp. 150–157.

[11] Gratt, H. J., McCowan, W. L., *Feedback Linearization Autopilot Design for the Advanced Kinetic Energy Missile Boost Phase,* Journal of Guidance, Control, and Dynamics, 5/1995, pp. 945–950.

[12] Ćuk, D., *Influence of Range Extension on Dynamic Stability for Artillery Rockets with Wrap Around Fins,* Military Technical Courier (Vojnotehnički glasnik), Ministry of Defence of the Republic of Serbia, vol. 55, No. 3, pp. 296–307, ISSN 0042-8469, UDC 623+355/359, Beograd 2007.

[13] Stengel, R. F., *Flight Dynamics,* Princeton University Press, 2004.

[14] Ćuk, D., *Choice of the Rotational Factor of the Thrust Vector for the Ballistic Missile with Lambert Guidance,* Military Technical Courier (Vojnotehnički glasnik), Ministry of Defence of the Republic of Serbia, vol. 56, No. 2, pp. 133–146, ISSN 0042-8469, UDC 623+355/359, Beograd 2008.

[15] Gregoriou, G., *CEP Calculation for a Rocket with Different Control System*, J. Guidance, 3/1988, pp. 193–198.

[16] Garnel, P., *Guided Weapon Systems,* Pergamon Press, New York, 1980.

POREĐENJE RAZLIČITIH AUTOPILOTA ZA UPRAVLJANJE NORMALNIM UBRZANJEM RAKETE ZEMLJA–ZEMLJA

OBLAST: Mašinstvo (Raketna tehnika)

Sažetak

Ovaj rad prikazuje poređenje tri autopilota za upravljanje normalnim ubrzanjem rakete zemlja–zemlja: konvencionalnog autopilota sa tri povratne sprege, i autopilota za upravljanje ugaonom brzinom vektora brzine i normalnim ubrzanjem koji su zasnovani na primeni inverznog dinamičkog upravljanja. Kretanje rakete zemlja–zemlja opisuje se nelinearnim diferencijalnim jednačinama čiji se parametri menjaju u širokom opsegu zbog promene brzine i visine leta. Zahtev za tačnim upravljanjem rakete u takvom okruženju predstavlja izazov za konstruktora autopilota. Dat je sažet pregled proračuna faktora pojačanja konvencionalnog autopilota primenom metode lokalne stabilnosti za linearni nestacionarni sistem sa „zamrznutim" dinamičkim koeficijentima. Metoda inverznog dinamičkog upravljanja prikazana je u narednom odeljku za dva tipa autopilota: za upravljanje ugaonom brzinom vektora brzine i normalnim ubrzanjem. Oba zahtevaju sintezu estimatora za veličine koje se koriste kao ulazne za zakon upravljanja raketom. Na kraju, pomoću modela „6-stepeni slobode kretanja" daju se rezultati simulacije odgovora rakete na zahtevanu komandu pri letu po tipičnoj balističkoj putanji. Poređenjem tri autopilota razmatraju se greške u stacionarnom stanju i osetljivost odgovora na izrazito promenljivo okruženje. Pokazano je da inverzno dinamičko upravljanje može da bude veoma efikasno u upravljanju raketom zemlja–zemlja.

Uvod

Nevođena raketa, koja je projektovana za domet od oko 50 km, modifikovana je u vođenu sa smanjenim rasturanjem. Za tako modifikovanu raketu neophodna je primena autopilota za upravljanje normalnim ubrzanjem kako bi se dobio zadovoljavajući odgovor rakete na svim visinama leta. Posle pregleda publikovanih radova iz oblasti raketne tehnike, daje se predmet ovog rada koji obuhvata analizu rezultata odgovora tri tipa autopilota rakete zemlja–zemlja: konvencionalnog autopilota ubrzanja sa tri povratne sprege i dva autopilota koji se zasnivaju na primeni inverznog dinamičkog upravljanja.

Konvencionalni autopilot ubrzanja sa tri povratne sprege

Data je sažeta sinteza autopilota ubrzanja sa tri povratne sprege za statički nestabilnu raketu. Primenom kvazistacionarne metode, sračunavaju se faktori pojačanja autopilota u zavisnosti od dinamičkih parametara leta rakete.

Sinteza autopilota primenom inverznog dinamičkog upravljanja

Posle opisa metode inverznog dinamičkog upravljanja, razmatrana su dva tipa autopilota: autopilot za upravljanje ugaonom brzinom vektora brzine i autopilot za upravljanje normalnim ubrzanjem pakete. Određena je struktura zakona upravljanja i uvedeni određeni estimatori veličina stanja. Izvedeni su svi potrebni izrazi za proračun faktora pojačanja i korekciju komande zbog nestacionarnosti parametara leta rakete.

Numerički primeri i simulacija

Verifikacija odabranih autopilota izvršena je numeričkom simulacijom odgovora rakete na datu komandu pomoću modela „6 stepeni slobode kretanja“. Pokazano je da primena konvencionalnog autopilota ubrzanja ne daje zadovoljavajuće rezultate zbog povećane statičke greške i prebačaja koji su funkcije parametara leta rakete. Suprotno tome, autopiloti koji su zasnovani na inverznom dinamičkom upravljanju daju željene odgovore nezavisno od promenljivih parametara leta rakete.

Zaključak

Sumirane su dinamičke osobine tri tipa autopilota: konvencionalnog autopilota ubrzanja sa tri povratne sprege, autopilota za upravljanje ugaonom brzinom tangente na putanju i autopilota za upravljanje normalnim ubrzanjem rakete. Poslednja dva zasnivaju se na primeni savremene metode upravljanja poznate kao inverzno dinamičko upravljanje. Faktori pojačanja konvencionalnog autopilota dodatno se podešavaju i verifikuju pomoću modela „6 stepeni slobode kretanja“. Suprotno tome, metoda inverznog dinamičkog upravljanja veoma je pogodna za dinamičke objekte sa jako promenljivim parametrima kakva je i raketa zemlja–zemlja. Zakon

upravljanja određuje se u prvom koraku za linearan stacionaran sistem, da bi se u drugom prolazu odredio otklon upravljačkih krila u zavisnosti od novog upravljačkog vektora i promenljivih dinamičkih parametara leta rakete. Primena inverznog dinamičkog upravljanja zahteva sintezu određenih estimatora veličina stanja rakete, koji bi bili predmet budućih istraživanja autopilota za rakete zemlja–zemlja.

Ključne reči: *autopilot, autopilot normalnog ubrzanja, autopilot ugaone brzine vektorom brzine, inverzno dinamičko upravljanje, vođena raketa zemlja–zemlja, model „6 stepeni slobode kretanja“.*

Datum prijema članka: 26. 01. 2011.

Datum dostavljanja ispravki rukopisa: 10. 02. 2011.

Datum konačnog prihvatanja članka za objavljivanje: 12. 02. 2011.